Evidence for a two-site localized hydrogen motion in C15-type YMn_2H_x

2006 J. Phys.: Condens. Matter 18 7249

(http://iopscience.iop.org/0953-8984/18/31/019)

INSTITUTE OF PHYSICS PUBLISHING JOURNAL OF PHYSICS: CONDENSED MATTER

J. Phys.: Condens. Matter **18** (2006) 7249–7256 doi:10.1088/0953-8984/18/31/019

Evidence for a two-site localized hydrogen motion in C15-type YMn_2H_x

A V Skripov[1], **M A Gonzalez**[2] **and R Hempelmann**[3]

[1] Institute of Metal Physics, Urals Branch of the Academy of Sciences, Ekaterinburg 620041, Russia
[2] Institut Laue–Langevin, F-38042 Grenoble, France
[3] Institut für Physikalische Chemie, Universität des Saarlandes, D-66041 Saarbrücken, Germany

Received 25 April 2006, in final form 26 June 2006
Published 21 July 2006
Online at stacks.iop.org/JPhysCM/18/7249

Abstract

In order to clarify the mechanism of the fast localized motion of hydrogen in the cubic (C15-type) Laves phase YMn_2, we have performed quasielastic neutron scattering measurements in YMn_2H_x ($x = 0.6$ and 1.2) over the temperature range 10–376 K. The behaviour of the elastic incoherent structure factor as a function of momentum transfer (studied up to $Q_{max} \approx 3$ Å^{-1}) is consistent with the two-site motion of H atoms within pairs of closely spaced interstitial g (Y_2Mn_2) sites. Comparison of the data for $YMn_2H_{0.6}$ and $YMn_2H_{1.2}$ shows that both the hydrogen jump rate and the fraction of H atoms participating in the fast localized motion decrease with increasing H content.

1. Introduction

Hydrogen diffusion in a number of cubic (C15-type) Laves-phase intermetallic compounds AB_2 shows two types of H jump motion with different characteristic frequencies [1]. The faster jump process corresponds to localized H motion over small groups of interstitial sites, and the slower process is responsible for the long-range H diffusion [2, 3]. The existence of the two frequency scales of H jump motion is believed to be related to the structure of the sublattice of interstitial sites partially occupied by hydrogen. In most of the cubic Laves-phase hydrides AB_2H_x, H atoms occupy only tetrahedral g sites (with $[A_2B_2]$ coordination) at low and intermediate hydrogen concentrations (up to $x \approx 2.5$), and tetrahedral e sites (with $[AB_3]$ coordination) start to be filled at higher H concentrations [4, 5]. The spatial arrangement of interstitial g and e sites in the C15-type lattice is shown in figure 1. In the following, we shall consider only the compounds with exclusive g-site occupation. As can be seen from figure 1, the sublattice of g sites consists of hexagons lying in the planes perpendicular to ⟨111⟩ directions. Each g site has three nearest neighbours: two g sites (on the same hexagon) at a distance r_1 and one g site (on the adjacent hexagon) at a distance r_2. The ratio r_2/r_1 is determined by the positional parameters (X_g and Z_g) of hydrogen atoms at g sites; these parameters are found to depend on the ratio of the metallic radii R_A and R_B of the elements A

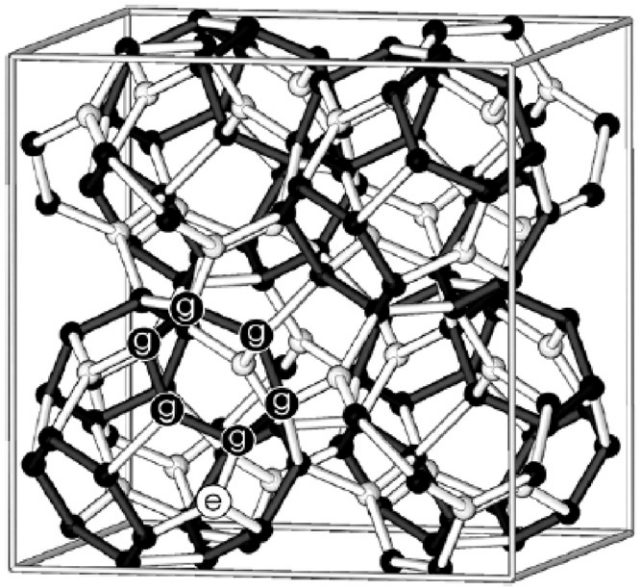

Figure 1. The spatial arrangement of interstitial g sites (dark spheres) and e sites (light spheres) in the C15-type lattice [6].

and B [1]. The microscopic picture of H motion has been investigated mostly for compounds with $R_A/R_B \leqslant 1.25$, where r_1 is shorter than r_2 [2, 3, 7–9]. For these compounds, the faster H jump process has been identified as the localized motion within the g-site hexagons.

For cubic Laves phases with $R_A/R_B > 1.35$, the g–g distance r_2 becomes shorter than r_1. This may lead to a qualitative change in the microscopic picture of H motion: the faster jump process is expected to be transformed into the back-and-forth jumps within *pairs* of g sites separated by r_2. In order to test this hypothesis, quasielastic neutron scattering (QENS) has been applied [10] to probe H motion in the cubic Laves phase YMn_2 with $R_A/R_B = 1.425$. While this study gave detailed information on the long-range H diffusion, no decisive conclusions about the nature of the localized H motion could be made [10] because of the following factors: (1) the long-range H diffusivity in YMn_2H_x appears to be unexpectedly high, so that it is difficult to separate the wings of the high-intensity narrow line (resulting from the long-range H diffusion) from the low-intensity broad line (resulting from the localized H motion) in the experimental QENS spectra, and (2) the range of the neutron momentum transfer in [10] is insufficient to distinguish unambiguously between different models of the localized H motion. The aim of the present work is to clarify the microscopic picture of the localized H motion in YMn_2. Therefore, the experimental parameters of the present QENS measurements are optimized for observation of the localized motion. In comparison with the previous QENS study [10], this means a higher maximum value of the neutron momentum transfer, a higher neutron intensity, and a poorer energy resolution. In the region of low hydrogen concentrations ($x \leqslant 1.2$), the YMn_2H_x system retains a paramagnetic solid solution state with the C15-type host-lattice structure down to 245 K; below this temperature a number of structural and magnetic phase transitions are known to occur [11]. In the present work we report the results of QENS measurements for YMn_2H_x ($x = 0.6$ and 1.2) over the temperature range 249–376 K. These measurements provide the first direct evidence for a two-site localized H motion in a cubic Laves-phase compound.

2. Experimental details

The preparation of YMn_2H_x samples was analogous to that described in [10]. According to x-ray diffraction analysis, at room temperature the samples were single-phase solid solutions of hydrogen in YMn_2 with the C15-type host-lattice structure and the lattice parameters $a = 7.781$ Å ($YMn_2H_{0.6}$) and 7.880 Å ($YMn_2H_{1.2}$).

QENS measurements were performed on the disc-chopper time-of-flight spectrometer IN5 at the Institute Laue–Langevin (ILL) in Grenoble. In addition to having a well-defined instrumental resolution function without long 'wings', this spectrometer allows one to optimize the experimental conditions by changing the incident neutron wavelength λ_i, the energy resolution and the neutron-beam intensity. In order to observe broad quasielastic lines originating from fast localized motion, it is necessary to have a high neutron intensity and a high maximum value of the elastic momentum transfer $\hbar Q$, but the energy resolution may be relatively low. On the basis of these considerations, we have chosen $\lambda_i = 3.6$ Å and a chopper speed of 12 000 revolutions per minute; such a choice results in an energy resolution of 0.22 meV (full width at half maximum) and a maximum Q-value of 3.19 $Å^{-1}$. For comparison, the maximum Q-value in [10] was 2.25 $Å^{-1}$. The powdered YMn_2H_x samples were placed into flat Al containers, the sample thickness being 0.5 mm. The plane of the container was oriented along the line $2\theta = 135°$ (the highest angle limit of the detector bank). QENS spectra $S_{exp}(Q, \omega)$, where $\hbar\omega$ is the energy transfer, were recorded at $T = 10$, 259, 283, 303, 322, 341, 359 and 372 K for $YMn_2H_{0.6}$ and at $T = 10$, 249, 278, 298, 317, 335, 358 and 376 K for $YMn_2H_{1.2}$. For data analysis, the detectors were binned into nine groups. The scattering angles corresponding to the Bragg reflections were excluded from the analysis. The raw experimental data were corrected for absorption and self-shielding using the standard ILL programs. The instrumental resolution functions $R(Q, \omega)$ were determined from the measured QENS spectra of YMn_2H_x at 10 K. The background spectra were measured for the empty sample containers in the same experimental geometry as for YMn_2H_x.

3. Results and discussion

Because of the very large incoherent scattering cross-section of hydrogen, the observed neutron scattering from our YMn_2H_x samples is dominated by the incoherent nuclear scattering on protons. QENS spectra measured at $T = 259$ K for $YMn_2H_{0.6}$ and at 249 K for $YMn_2H_{1.2}$ can be satisfactorily described by a sum of two components: an 'elastic' line represented by the spectrometer resolution function and a resolution-broadened Lorentzian 'quasielastic' line. The relative intensity of the 'quasielastic' component is found to increase with increasing Q, its half-width being nearly Q-independent. These features are typical of the case of spatially restricted (localized) motion [12, 13]. However, at higher temperatures the description in terms of a sum of an elastic line and a single Lorentzian quasielastic component leads to systematic deviations of the model QENS spectra from the experimental spectra. For $T > 260$ K, we have to add the second Lorentzian quasielastic component, so that the experimental scattering function $S_{exp}(Q, \omega)$ is fitted with the model incoherent scattering function

$$S_{inc}(Q, \omega) = A_0(Q)\delta(\omega) + A_1(Q)L(\omega, \Gamma_1) + A_2(Q)L(\omega, \Gamma_2) \tag{1}$$

convoluted with $R(Q, \omega)$. Here, $\delta(\omega)$ is the elastic δ-function, $L(\omega, \Gamma)$ is the Lorentzian function with the half-width Γ, and $A_0 + A_1 + A_2 = 1$. A similar description of the time-of-flight QENS spectra was used in our previous work [10]. As an example of the data, figure 2 shows the QENS spectrum of $YMn_2H_{1.2}$ recorded at 298 K for $Q = 2.79$ $Å^{-1}$.

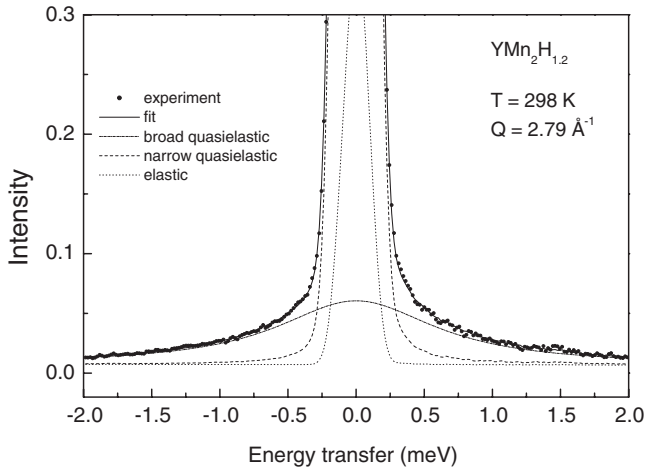

Figure 2. The QENS spectrum for $YMn_2H_{1.2}$ measured on IN5 at $T = 298$ K and $Q = 2.79$ Å^{-1}. The full curve shows the fit of the three-component model (equation (1)) to the data. The dotted curve represents the elastic component (the spectrometer resolution function) and the broken curves show two Lorentzian quasielastic components.

At the first stage of the analysis, we have used the model function (1) with two amplitudes (A_0, A_1, $A_2 = 1 - A_0 - A_1$) and two half-widths (Γ_1, Γ_2) being independent fit parameters. Qualitatively, the results of such an analysis are similar for both $YMn_2H_{0.6}$ and $YMn_2H_{1.2}$. The intensity of the broader quasielastic component, $A_2(Q)$, is found to increase with increasing Q, and its half-width Γ_2 appears to be nearly Q-independent. Since these features are typical of a spatially confined motion [12, 13], the broad quasielastic component can be attributed to the fast localized H motion with the jump rate τ_1^{-1}. In this case, the value of Γ_2 is proportional to τ_1^{-1}, and the Q-dependence of A_2 is related to the geometry of this motion. It should be noted that the observed monotonic increase of A_2 with increasing Q up to $Q_{max} \approx 3$ Å^{-1} and the increase of A_2 with increasing temperature exclude the possibility that the broader quasielastic component originates from magnetic fluctuations in the paramagnetic phase. Hence, the magnetic quasielastic neutron scattering for our samples in the temperature range studied appears to be much weaker than the nuclear quasielastic neutron scattering (dominated by scattering on protons). The narrow quasielastic line is the most intense component of the spectra. Its half-width Γ_1 is found to increase with increasing Q, reaching a saturation in the Q-range 1.6–2.2 Å^{-1}. Furthermore, the value of Γ_1 increases strongly with increasing temperature. These features suggest that the narrow quasielastic component originates from a jump process leading to the long-range diffusion of hydrogen. The intensity of the elastic component, A_0, is found to be small (about 10% of the total scattered intensity), being nearly Q-and T-independent. This component can be attributed to the residual elastic contribution resulting mainly from the scattering by host-metal nuclei.

As the next step of the analysis, at a given temperature we have simultaneously fitted the spectra for all Q with equation (1), assuming a common value of Γ_2 and a fixed A_0 (being equal to its average value in individual fits). In this case, the fit parameters are Γ_2 (common value for all Q), A_1 and Γ_1 (individual values for each Q). The resulting fit of the three-component model to the data at $T = 298$ K and $Q = 2.79$ Å^{-1} is shown by the full curve in figure 2; the broken curves represent contributions of the different components. The Q- and T-dependences of Γ_1 derived from the fit are close to those obtained in the previous work [10], where the

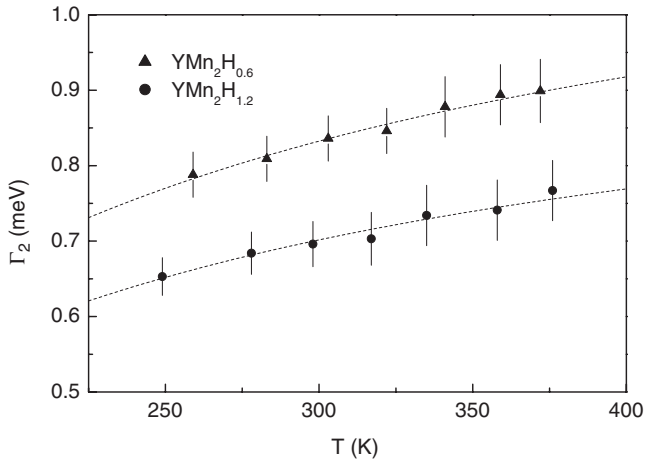

Figure 3. The temperature dependences of the half-width of the broader quasielastic line for $YMn_2H_{0.6}$ and $YMn_2H_{1.2}$. The dashed curves show the Arrhenius fits to the data.

parameters of the long-range H diffusion resulting from these dependences for YMn_2H_x with low x have been discussed in detail. In the present work, we focus on the behaviour of the broader quasielastic component related to the localized H motion.

Figure 3 shows the temperature dependences of the half-width Γ_2 derived from the fits of the three-component model to the data for $YMn_2H_{0.6}$ and $YMn_2H_{1.2}$. It can be seen that the half-width increases with increasing temperature, the values of Γ_2 for $YMn_2H_{0.6}$ being higher than the corresponding values for $YMn_2H_{1.2}$. This means that the characteristic jump rate of the localized H motion increases with increasing temperature and decreases with increasing hydrogen content. A similar behaviour of the jump rate has been found for the localized H motion in C15-type TaV_2H_x [2] and $ZrMo_2H_x$ [7]. The dashed lines in figure 3 show the Arrhenius fits to the data. The values of the activation energies resulting from the fits are 10 ± 3 meV for both $YMn_2H_{0.6}$ and $YMn_2H_{1.2}$. These activation energies characterizing the localized H motion are much lower than those for the long-range H diffusion in YMn_2H_x (for example, the activation energy for the long-range H diffusion in $YMn_2H_{0.65}$ is 213 ± 5 meV [10]). Similar difference in the activation energies of the two H jump processes has also been found for other Laves-phase hydrides [1, 8, 9]. It should be noted, however, that the observed range of Γ_2 variations in our experiments is too small to verify if the temperature dependence of Γ_2 is in fact described by the Arrhenius law.

The geometry of the localized H motion can, in principle, be derived from the Q-dependence of the elastic incoherent structure factor (EISF) [12, 13]. Assuming that the purely elastic component of QENS spectra described by equation (1) originates from the host-metal contribution, we can determine the 'resolution-limited' EISF for the hydrogen sublattice as the ratio $A_1/(A_1 + A_2)$. Figure 4 shows the Q-dependence of the EISF for $YMn_2H_{1.2}$ at three temperatures. Similar behaviour of the EISF is observed for $YMn_2H_{0.6}$. Note that the results shown in figure 4 correspond to the changes in the *relative* intensity of the narrow component, not to the changes in the absolute intensity with Q and T. As can be seen from figure 4, the measured EISF appears to be temperature-dependent, decreasing with increasing T. This feature is common for all the studied Laves-phase hydrides [1–3, 7–9]. In order to account for this feature, we have to assume that only a fraction p of the H atoms participates in the fast localized motion, and this fraction increases with temperature. The existence of 'static'

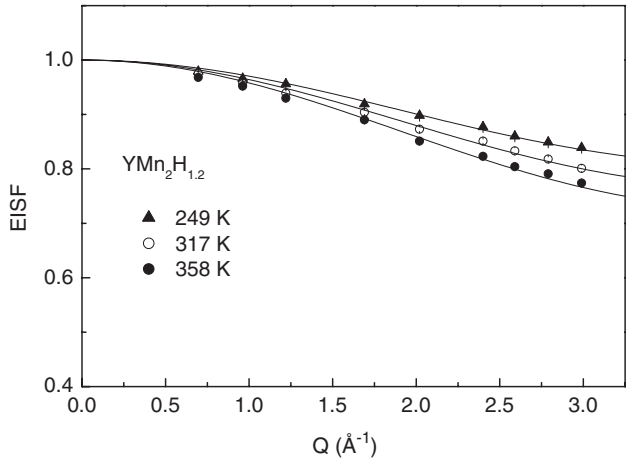

Figure 4. The elastic incoherent structure factor for $YMn_2H_{1.2}$ as a function of Q measured at $T = 249$, 317 and 358 K. The full curves show the fits of the two-site model (equation (3)) with the fixed $r_2 = 1.09$ Å to the data.

H atoms may result from the H–H interaction leading to formation of some ordered atomic configurations at low temperatures [2].

According to neutron diffraction measurements [14], at room temperature the D atoms in YMn_2D_x with $x \leqslant 3.4$ occupy only g sites with the positional parameters $X_g = 0.324$–0.327 and $Z_g = 0.137$–0.141. The structure of the g-site sublattice (see figure 1) suggests two possible types of localized H motion. The first possibility is that a hydrogen atom jumps over six g sites, forming a regular hexagon with the nearest-neighbour g–g distance r_1. This type of localized motion has been observed in a number of cubic Laves-phase hydrides [2, 3, 7–9]. The second possibility corresponds to back-and-forth jumps between two g sites separated by r_2. For the six-site model, the orientationally averaged form of the EISF [12, 13] is given by

$$\mathrm{EISF} = 1 - p + \frac{p}{6}[1 + 2j_0(Qr_1) + 2j_0(Qr_1\sqrt{3}) + j_0(2Qr_1)], \tag{2}$$

where $j_0(x)$ is the spherical Bessel function of zeroth order. For the two-site model, the Q-dependence of the orientationally averaged EISF [12, 13] is given by

$$\mathrm{EISF} = 1 - p + \frac{p}{2}[1 + j_0(Qr_2)]. \tag{3}$$

Note that the period of the oscillatory Q-dependence of the EISF described by equations (2) and (3) is determined by the corresponding intersite distances (r_1 or r_2), while the value of p is responsible only for the amplitude of these oscillations. Using the experimental positional parameters of D atoms in $YMn_2D_{1.0}$ ($X_g = 0.326$, $Z_g = 0.141$) [14] to calculate g–g distances in YMn_2H_x, we find that, for $YMn_2H_{1.2}$, $r_1 = 1.40$ Å and $r_2 = 1.09$ Å. Comparison of the experimental Q-dependences of the EISF with the models represented by equations (2) and (3) indicates that only the two-site model is consistent with the data. Figure 5 shows the fit of the two-site model (equation (3), full curve) with the fixed $r_2 = 1.09$ Å to the EISF data for $YMn_2H_{1.2}$ at the highest T studied (at which the range of the EISF variation is the widest). It can be seen that equation (3) with p as the only fit parameter satisfactorily describes the observed Q-dependence of the EISF. The value of p resulting from the fit is 0.486 ± 0.004. The two-site model with the fixed $r_2 = 1.09$ Å also gives a reasonable description of the EISF data at the other temperatures (see, for example, the full curves in figure 4) as well as the EISF data for

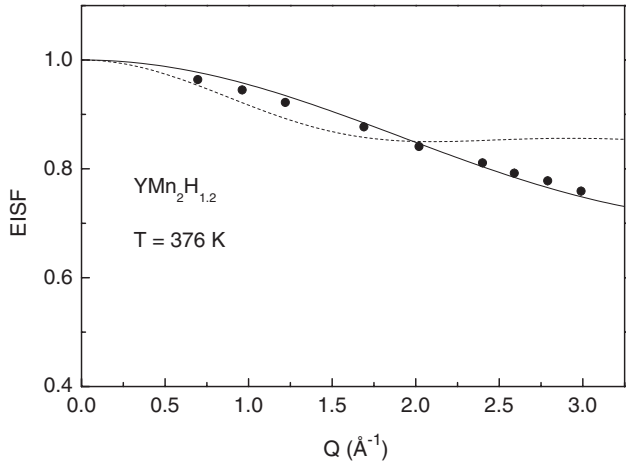

Figure 5. The elastic incoherent structure factor for $YMn_2H_{1.2}$ at 376 K as a function of Q. The full curve shows the fit of the two-site model (equation (3)) with the fixed $r_2 = 1.09$ Å to the data. The dashed curve shows the behaviour of the EISF predicted by the six-site model (equation (2)) with the fixed $r_1 = 1.40$ Å.

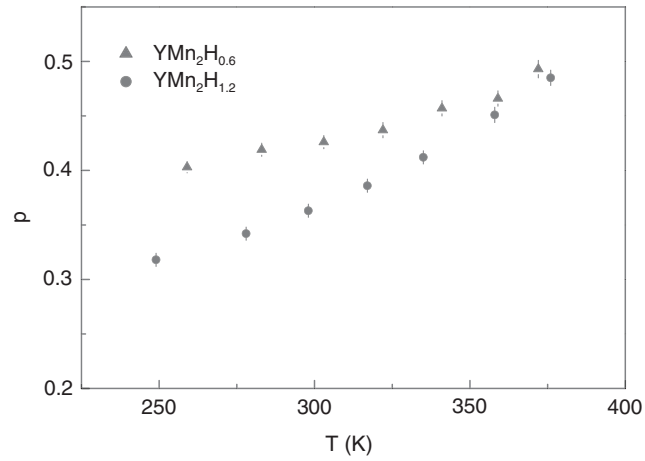

Figure 6. The temperature dependences of the fraction of H atoms participating in the fast localized motion, as determined from the fits of the two-site model to the data for $YMn_2H_{0.6}$ and $YMn_2H_{1.2}$.

$YMn_2H_{0.6}$. The dashed curve in figure 5 shows the behaviour predicted by the six-site model (equation (2)) with the fixed $r_1 = 1.40$ Å. It can be seen that, in the Q-range 2.0–3.2 $Å^{-1}$, the six-site model predicts the increase of EISF with increasing Q, whereas the experimental EISF *decreases* in this range. Thus, the six-site model is inconsistent with the observed Q-dependence of the EISF. It should be noted that QENS measurements at $Q > 2.3$ $Å^{-1}$ are crucial for such a conclusion.

Figure 6 shows the temperature dependences of p resulting from the fits of the two-site model to the EISF data for $YMn_2H_{0.6}$ and $YMn_2H_{1.2}$. The fraction of H atoms participating in the fast localized motion appears to decrease with increasing H content, especially at low temperatures. This is consistent with the idea that H–H interactions tend to suppress the fast localized motion.

4. Conclusions

The analysis of our quasielastic neutron scattering data for C15-type YMn_2H_x ($x = 0.6$ and 1.2) has shown that the fast H jump process in this system corresponds to localized motion of H atoms within pairs of closely spaced g sites. This is the first unambiguous evidence for a two-site localized hydrogen motion in a Laves-phase compound. The observation of the two-site H motion provides the 'missing link' for the systematics of hydrogen jump processes in cubic Laves-phase hydrides [1]; it shows that the change in the structure of the g-site sublattice (corresponding to the transition from $r_2 > r_1$ to $r_2 < r_1$) leads to the qualitative change in the microscopic picture of H motion.

Acknowledgments

The authors are grateful to J Ollivier for assistance with the QENS measurements at ILL. This work was supported by the Russian Foundation for Basic Research (Grant No 06-02-16246) and the Priority Programme 'Hydrogen Energy' of the Russian Academy of Sciences. AVS also acknowledges financial support from the Universität des Saarlandes.

References

[1] Skripov A V 2003 *Defect Diffus. Forum* **224/225** 75
[2] Skripov A V, Cook J C, Sibirtsev D S, Karmonik C and Hempelmann R 1998 *J. Phys.: Condens. Matter* **10** 1787
[3] Skripov A V, Pionke M, Randl O and Hempelmann R 1999 *J. Phys.: Condens. Matter* **11** 1489
[4] Somenkov V A and Irodova A V 1984 *J. Less-Common Met.* **101** 481
[5] Yvon K and Fischer P 1988 *Hydrogen in Intermetallic Compounds I* ed L Schlapbach (Berlin: Springer) p 87
[6] Eberle U, Majer G, Skripov A V and Kozhanov V N 2002 *J. Phys.: Condens. Matter* **14** 153
[7] Skripov A V, Cook J C, Karmonik C and Kozhanov V N 1999 *Phys. Rev.* B **60** 7238
[8] Skripov A V, Cook J C, Udovic T J and Kozhanov V N 2000 *Phys. Rev.* B **62** 14099
[9] Bull D J, Broom D P and Ross D K 2003 *Chem. Phys.* **292** 153
[10] Skripov A V, Cook J C, Udovic T J, Gonzalez M A, Hempelmann R and Kozhanov V N 2003 *J. Phys.: Condens. Matter* **15** 3555
[11] Figiel H, Przewoznik J, Paul-Boncour V, Lindbaum A, Gratz E, Latroche M, Escorne M, Percheron-Guégan A and Mietniowski P 1998 *J. Alloys Compounds* **274** 29
[12] Bée M 1988 *Quasielastic Neutron Scattering* (Bristol: Hilger)
[13] Hempelmann R 2000 *Quasielastic Neutron Scattering and Solid State Diffusion* (Oxford: Clarendon)
[14] Latroche M, Paul-Boncour V, Przewoznik J, Percheron-Guégan A and Bourée-Vigneron F 1995 *J. Alloys Compounds* **231** 99